Received: 16 November 2022 | Accepted: 21 November 2022

DOI: 10.1002/psp4.12898

ARTICLE

Oncolytic viral kinetics mechanistic modeling of Talimogene Laherparepvec (T-VEC) a first-in-class oncolytic viral therapy in patients with advanced melanoma

Malidi Ahamadi[1] | **Johannes Kast**[2] | **Po-Wei Chen**[1] | **Xiaojun Huang**[3] | **Sandeep Dutta**[1] | **Vijay V. Upreti**[2]

[1]Clinical Pharmacology Modeling and Simulation, Amgen Inc, Thousand Oaks, California, USA

[2]Clinical Pharmacology Modeling and Simulation, Amgen Inc, South San Francisco, California, USA

[3]Global Development, Amgen Inc, Thousand Oaks, California, USA

Correspondence
Malidi Ahamadi, Clinical Pharmacology Modeling and Simulation, Amgen Inc, Thousand Oaks, CA 91320, USA.
Email: mahamadi@amgen.com

Abstract

Talimogene Laherparepvec (T-VEC) is a first-in-class oncolytic virotherapy approved for the treatment of unresectable melanoma recurrent after initial surgery. Biodistribution data from a phase II study was used to develop a viral kinetic mechanistic model describing the interaction between cytokines such as granulocyte-macrophage colony-stimulating factor (GM-CSF), the immune system, and T-VEC treatment. Our analysis found that (1) the viral infection rate has a great influence on T-VEC treatment efficacy; (2) an increase in T-VEC dose of 10^2 plaque-forming units/ml 21 days and beyond after the initial dose of T-VEC resulted in an ~12% increase in response; and (3) at the systemic level, the ratio of resting innate immune cells to the death rate of innate immune impact T-VEC treatment efficacy. This analysis clarifies under which condition the immune system either assists in eliminating tumor cells or inhibits T-VEC treatment efficacy, which is critical to both efficiently design future oncolytic agents and understand cancer development.

Study Highlights

WHAT IS THE CURRENT KNOWLEDGE ON THE TOPIC?

T-VEC is a first-in-class oncolytic virotherapy approved for the treatment of unresectable melanoma recurrent after initial surgery. However, there is a lack of a comprehensive quantitative approach that systematically evaluates T-VEC efficacy.

WHAT QUESTION DID THIS STUDY ADDRESS?

This analysis (i) developed a viral kinetic mechanistic model in melanoma patients leveraging T-VEC clinical data, (ii) identified model parameters that influence T-VEC treatment efficacy and immune response, and (iii) quantified the correlation between a T-VEC dose/dosing regimen and the time course of anti-melanoma tumor response.

WHAT DOES THIS STUDY ADD TO OUR KNOWLEDGE?

This platform model adequately captures the well-known, complex, multifaceted mechanism of action of T-VEC and identifies under which condition the immune system either assists in eliminating tumor cells or inhibits T-VEC efficacy.

HOW MIGHT THIS CHANGE DRUG DISCOVERY, DEVELOPMENT, AND/OR THERAPEUTICS?

This mechanistic platform model can be used as quantitative knowledge based to efficiently inform clinical trials and for the design of future oncolytic agents.

INTRODUCTION

Oncolytic viruses are an emerging class of immunotherapies that promote tumor regression by attacking and infecting cancerous cells and stimulate the host antitumor immunity. However, depending on the degree of severity of the viral infection, the host immune system can act both as a barrier and facilitator.[1–4] Thus, one of the challenges when designing oncolytic virotherapy is how to optimize the complex dynamic between antiviral responses, viral clearance, and immune-mediated tumor destruction. Granulocyte-macrophage colony-stimulating factor (GM-CSF) is a white blood cell growth factor responsible for stimulating granulocyte production and is known to have a variety of effects on the immune system, including the activation of T cells and the maturation of dendritic cells.[5–8] Talimogene Laherparepvec (T-VEC) is a first-in-class oncolytic virotherapy approved for the treatment of unresectable melanoma recurrent after initial surgery.[3] T-VEC is a genetically engineered herpes simplex virus type 1 that selectively replicates in tumor tissue and lyses tumor cells while promoting antitumor immunity.[3] To further enhance T-VEC immunogenicity, two copies of the human *GM-CSF* gene were inserted into the virus genome to enhance the influx of dendritic cells into the tumor and their activation.[3,9] Initial tolerability of T-VEC has been established in a phase I trial of 30 patients with refractory cutaneous or subcutaneous metastases from melanoma, breast cancer, gastrointestinal adenocarcinoma, or squamous cell carcinoma of the head and neck.[10] Local reactions were found to be dose limiting at 10^7 plaque-forming units (pfu)/ml, but did not influence T-VEC efficacy. Pfu is a metric measuring the quantity of viruses that are capable of lysing host cells and forming a plaque. Numerous studies exist in the literature that assess and review T-VEC efficacy and safety.[10–13] Andtbacka et al.[11] evaluated T-VEC DNA biodistribution, shedding, and its potential transmission during and after completion of therapy in adults with advanced melanoma using data from a phase II, single-arm, open-label study. Their analysis confirmed that T-VEC can be administered safely to patients with advanced melanoma and is unlikely to be transmitted to close contacts with the appropriate use of occlusive dressings. T-VEC response rate was reported to be 35%, including 15% with complete response (CR) and 20% with partial response. Furthermore, 17% of patients were reported with stable disease (SD) and 26% with progressive disease (PD). A further detailed T-VEC response rate was evaluated in the Oncovex(GM-CSF) Pivotal Trial in Melanoma (OPTiM) clinical trial and reported in Andtbacka et al.[13] To our best knowledge, no mechanistic model that robustly quantifies T-VEC viral kinetic and describes the complex interactions between immune response and T-VEC treatment efficacy has been developed to date. Therefore, the aims of the current analysis were to (1) develop a viral kinetic mechanistic model in melanoma patients leveraging T-VEC clinical data, (2) identify model parameters that influence T-VEC treatment efficacy and immune response, and (3) quantify the correlation between dose/dosing regimen and the time course of melanoma.

Several mathematical models are published in the literature that describe the dynamics of oncolytic viruses and tumor cells.[14–21] Mahasa et al.[14] developed a mathematical model describing the interactions between the oncolytic virus, tumor cells, normal cells, and antitumoral and antiviral immune responses. Their analysis suggested that designing an oncolytic virus that is not 100% tumor specific can increase virus particles, which in turn can infect more tumor cells. Storey et al.[15] developed a mathematical model to describe the interactions between distinct populations of immune cells by incorporating both innate and adaptive immune responses to oncolytic viral therapy treating glioblastoma. Their analysis found that a stronger innate immune system leads to less effectiveness due to more rapid viral clearance by macrophages and natural killer cells. None of the existing mathematical models considers how the interaction between GM-CSF and both innate and adaptive immune responses influence oncolytic viral therapy.

T-VEC has a complex life cycle starting from manufacturing to clinical application compared with traditional small molecules or protein therapies. These factors pose great challenges in applying traditional pharmacometrics modeling and simulation approaches to evaluate T-VEC treatment efficacy. Here, T-VEC biodistribution data from a phase II study (NCT02014441) were used to quantify its response profile using a nonlinear mixed-effect model.

METHODS

Summary of clinical data

The modeling dataset was based on biodistribution data from a phase II, single-arm, open-label study (NCT02014441) that evaluated the biodistribution and shedding of T-VEC in patients with unresected stage IIIB to IVM1c melanoma. The primary objective of the study was to estimate the proportion of patients with detectable T-VEC DNA in the blood and urine. Key eligibility criteria included men or women aged ≥ 18 years with a histologically confirmed diagnosis and unresected stage IIIB, IIIC, IVM1a, IVM1b, or IVM1c melanoma regardless of prior line of therapy. Further details on inclusion/exclusion are reported elsewhere.[12] In this study, 60 patients were injected with T-VEC intralesional with an initial dose of 10^6 pfu/ml (up to 4 ml total injection volume based on lesion size) on study Day 1 followed by 10^8 pfu/ml (up to 4 ml total injection volume based on lesion size) 21 days after the initial dose and every 14 (±3) days thereafter. The injected lesions were covered with occlusive dressings for ≥1 week. Patients were treated with T-VEC until the achievement of CR or the disappearance of all injectable tumors. Samples from blood, urine, the exterior of occlusive dressings, and the surface of injected lesions were collected at multiple timepoints. Specifically, during Cycle 1 samples were collected on Day 1 before and approximately 1, 4, and 8 h after T VEC administration and on Days 2, 3, 8, and 15. During Cycle 2 samples were collected on Day 1 before and approximately 1, 4, and 8 hours after T-VEC administration and on Days 2, 3, and 8. During Cycle 3 samples were collected on Day 1 (before T-VEC administration) and Day 8. During Cycle 4 samples were collected on Day 1 (before T-VEC administration). Finally samples were collected at 30-day safety follow-up visit (see also Figure S1). The collected samples were used to evaluate the biodistribution and shedding of T-VEC during the treatment period and safety follow-up. The biodistribution of T-VEC in blood and all other tissues was evaluated using a validated quantitative polymerase chain reaction assay. Only T-VEC biodistribution data on the surface of injected lesions were used in this analysis as T-VEC DNA on the surface of the injected lesions was found to be maximally correlated with T-VEC exposure at the lesion level (site of action).[12] Efficacy end points included best overall response, objective response rate (CR or PR, according to modified World Health Organization criteria), and durable response rate (CR or PR for ≥6 months). The protocol was approved by the institutional review boards at each site, and all patients provided written informed consent before the start of any study-related procedures.[12]

Model structure

The viral kinetic mechanistic model includes the well-known multifaceted mechanisms of action of oncolytic viral therapy[14,15] and incorporates specific characteristics of T-VEC, such as the interaction between GM-CSF and innate

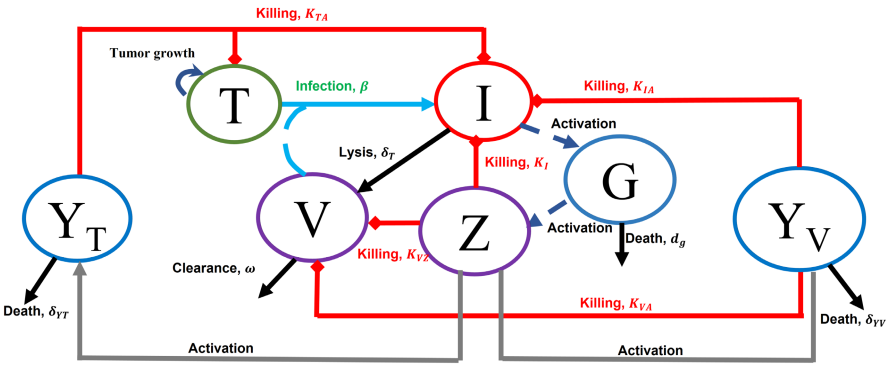

FIGURE 1 Structural model. δ_T, death rate of infected tumor cells, δ_{YV}, death rate of virus-specific adaptive immune cells; δ_{YT}, death of tumor-specific adaptive immune cells; d_g, GM-CSF clearance; G, total number of granulocyte-macrophage colony-stimulating factor; I, infected tumor cells; K_I, killing rate of infected cells by innate immune cells; K_{IA}, killing rate of infected cells by virus-specific adaptive immune cells; K_{TA}, killing rate of tumor cells by tumor-specific adaptive immune cells; K_{VA}, killing rate of T-VEC virions by virus-specific adaptive immune cells; K_{VZ}, killing rate of T-VEC virions by innate immune cells; V, talimogene laherparepvec virions; ω, viral clearance rate; and Z, innate immune cells.

and adaptive immune responses to T-VEC therapy. The final structural model, as shown in Figure 1, includes seven compartments that describe the longitudinal change of total number of (1) susceptible tumor cell population (T), (2) infected tumor cell population (I), (3) T-VEC virions (V), (4) GM-CSF (G), (5) innate immune cells (Z), (6) tumor-specific immune cells (Y_T), and (7) virus-specific immune cells (Y_V). The interaction between the different compartments is as follows: the susceptible tumor cells grow logistically at the rate intrinsic tumor cell growth rate until they reach their capacity tumor cell carrying capacity. Susceptible tumor cells get infected by the oncolytic virus with the viral infection rate β, transforming tumor cells from the susceptible population to the infected population. Following successful viral replication within the infected cells, apoptotic infected tumor cells lyse and release tumor-derived antigens. GM-CSF proliferates after encountering the virus from the infected cells. GM-CSF then activates innate immune cells, consisting of both macrophages and natural killer cells. Innate immune cells target and kill both viral particles and infected cells. The innate immune cells recruit the adaptive immune system that contains tumor-specific immune cells, and virus-specific immune cells. The tumor-specific immune cells, inhibit tumor and infected cells, whereas the virus-specific immune cells, inhibit both the T-VEC virion and infected tumor cells. Details about the model equations can be found in the supplemental material. The inclusion of the immune response component in the current viral kinetic model led to a highly nonlinear and overparametrized model, making the estimations of all model parameters practically impossible with the available T-VEC biodistribution data. The longitudinal tumor volume measurements were not available for the model development. A dual approach was used to evaluate the model parameters. Most of the model parameters describing intrinsic properties of the immune system were taken from the literature (see Data S1: Table A1). The remaining parameters related to T-VEC treatment efficacy were estimated using nonlinear mixed-effects modeling to account for the inherent variability of the T-VEC biodistribution data.

Model-building process

The viral kinetic mechanistic model was built using a nonlinear mixed-effect modeling approach in NONMEM version 7.4 (ICON Development Solutions). To capture the interindividual variability of T-VEC biodistribution, an exponential variability model was used. This was implemented by testing interindividual variability for each model parameter followed by an inspection of the correlations among the random-effect values to guide the development of a parsimonious covariance matrix structure. The predictive performance of the final population model was assessed using a visual predictive check approach. A total of 500 simulated data sets were generated using the final model. The observed biodistribution data were graphically overlaid with the median values and the 5th and 95th percentiles of the simulated biodistribution–time profiles. The performance of the model was deemed adequate if the observed biodistribution data were appropriately distributed within the 5th and 95th percentiles of the simulated data.

Global sensitivity analysis

Global sensitivity analysis was performed using the Latin hypercube sampling (LHS) and partial rank correlation coefficient (PRCC) analysis described by Chalom et al.[22] and implemented in R software package pse.[23] The first step of the algorithm was to determine the distribution of each model parameter. This is achieved by using following steps: (1) for model parameters that are fixed, their distribution was obtained by uniform sampling using the ranges provided in Data S1: Table A1; (2) for those that are estimated without interindividual variability, their distribution was generated by uniform sampling in a reasonable range based on biological information; and (3) for those that are estimated with interindividual variability, their distribution was obtained by sampling from normal distribution with the population mean and variance of the estimated model parameters. The second step was to generate a simulated virtual population treated with T-VEC. A total of 500 virtual patients, each with distinct tumor sizes and immune characteristics, were treated with T-VEC for 1, 2, and 4 months and sampled from the described distributions. The different T-VEC treatment durations were chosen to evaluate if and which model parameters depend on the length of the clinical trial. In each of the three simulated clinical trials (i.e., 1, 2 and 4 months), virtual patients were dosed 10^6 pfu/ml (up to 4 ml total injection volume) on study Day 7, followed by 10^8 pfu/ml (up to 4 ml total injection volume) on Days 21 and 28. The final step was to perform the sensitivity analysis using LHS/PRCC as implemented in the R software package pse.[22]

Simulations predicting T-VEC treatment efficacy

Monte Carlo–based clinical trial simulations were performed to showcase the ability of the current viral kinetic mechanistic model to predict T-VEC treatment efficacy. Virtual populations of 250, 500, and 1000 patients were generated to reflect both patient variability and the heterogenous nature of patient cohorts. Virtual individuals

were created by sampling each model parameter from distributions obtained from NONMEM estimations or from the literature for those parameters that were not estimated. To assess T-VEC efficacy, one clinical trial was simulated with a "lower dose" and one with a "higher dose" regimen in which each virtual patient was treated for 6 months: (1) the lower dose regimen consisted of an initial dose of 10^6 pfu/ml (up to 4 ml total injection volume) on study Day 7, followed by additional doses of 10^6 pfu/ml 21 days after the initial dose and on Days 33, 49, 63, 77, 91, 105, 119, 133, 147, and 161; (2) the "higher dose" regimen consisted of an initial dose of 10^6 pfu/ml (up to 4 ml total injection volume) on study Day 7, followed by 10^8 pfu/ml (up to 4 ml total injection volume) 21 days after the initial dose and on Days 33, 49, 63, 77, 91, 105, 119, 133, 147, and 161. Simulated tumor burden was defined as the sum of all infected cells in the tumor scaled by 10^{-6}, that is, (T + I) * 10^{-6}, assuming that 1 mm^3 of tumor burden contains 10^6 tumor cells.[3] Percentage change from baseline (defined as tumor burden measurement at Day 7) was calculated, and the ability of the model to predict T-VEC treatment efficacy was evaluated by comparing the percentage of virtual patients falling into each Response Evaluation Criteria in Solid Tumors (RECIST) category:[24] that is, responders including CR/PR, SD, and PD for each dose regimen (i.e., lower dose and higher dose). According to the RECIST criteria, PD was defined as a percentage change from baseline in tumor burden ≥20%, SD was defined as a >20% percentage change from baseline in tumor burden ≥−30%, and PR/CR were defined as a −30% > percentage change from baseline in tumor burden.[24]

RESULTS

In total, 360 T-VEC DNA samples based only on biodistribution data from the surface of injected lesions were analyzed. Incidence of quantifiable T-VEC DNA on the surface of injected lesions was found to be highest during Cycles 1 and 2 with peak DNA observed on Day 7 and Day

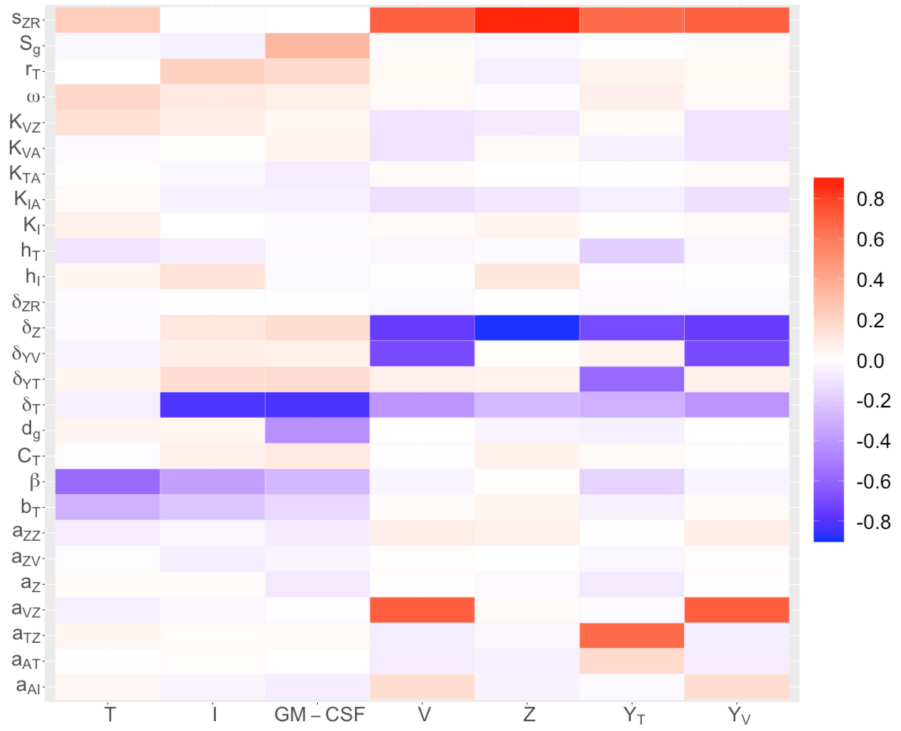

FIGURE 2 Global sensitivity analysis. a_{AI}, rate of infected cell mediated proliferation of virus specific adaptive immune cells; a_{AT}, rate of tumor cell mediated proliferation of tumor specific adaptive immune cells; a_{TZ}, activation rate of tumor specific adaptive immune cells via immune cells; a_{ZV}, virus mediated activation rate of resting innate immune cells; a_{ZZ}, activation of resting innate cells by previously activated innate immune cells; b_T, burst size of infected cells; β, viral infection rate; C_T, tumor cells carrying capacity; d_g, GM-CSF clearance; δ_T, death rate of infected tumor cells; δ_{YT}, death rate of tumor specific adaptive immune cells; δ_{YV}, death rate of virus specific adaptive immune cells; δ_Z, death rate of innate immune cells; δ_{ZR}, death rate of resting innate immune cells; GM-CSF, granulocyte-macrophage colony-stimulating factor; h_I, half saturation constant of infected tumor cells; h_T, half saturation constant of tumor cells; I, infected tumor cells; K_I, killing rate of infected cells by innate immune cells; K_{IA}, killing rate of infected cells by virus specific adaptive immune cells; K_{TA}, killing rate of tumor cells by tumor specific adaptive immune cells; K_{VA}, killing rate of T-VEC virions by virus-specific adaptive immune cells; K_{VZ}, killing rate of T-VEC virions by innate immune cells; r_T, intrinsic tumor cell growth rate; S_g, GM-CSF proliferation rate; S_{ZR}, source of the resting innate immune cells; V, Talimogene Laherparepvec virions; and ω, viral clearance rate.

22. Figure S1 describes the viral kinetics of T-VEC on the surface of injected lesions.

Seven model parameters from which five were linked to the dynamics of tumor burden (i.e., tumor cell growth rate, viral infection rate, death rate of infected tumor cells, and viral clearance rate) and two related to the immune system (i.e., killing rate of viruses by virus-specific immune cells and killing rate of viruses by innate immune cells) could be estimated. Interindividual variability could be assessed on tumor cell growth rate, viral infection rate, death rate of infected tumor cells, and viral clearance rate. Exploration of various residual variability models led to the selection of the combined residual error model on the log-scale, as this optimally characterized the distribution of residuals across the T-VEC biodistribution range. The final model was stable on perturbation of initial parameter estimates. The estimated model parameters are shown in Table S1, and model validation and goodness-of-fit plots are provided in Figures S2 and S3. It is noteworthy to mention that the scatter plots of population predicted versus observed T-VEC DNA concentrations shown in Figure S2B exhibit a bias, and the visual predictive check shown in Figure S3 suggests underprediction at the high percentiles of T-VEC DNA. These model-fitting challenges could be attributed to the fact that only the T-VEC distribution data were available for the development of the model.

Global sensitivity analysis

The heatmap presented in Figure 2 summarizes the overall degree of sensitivity between model outputs and model parameters after 4 months of treatment. The PRCC values range from −1 to 1, in which negative values characterize a negative effect and positive values denote a positive effect. The color in the vertical strip represents the degree of sensitivity, and an absolute value of PRCC above 0.5 was considered clinically significant. T-VEC viral infection rate β had the strongest sensitivity on susceptible tumor cells, whereas the death rate of infected tumor cells had the strongest sensitivity on both infected tumor cells and GM-CSF levels. These findings suggest that an increase of infection of susceptible tumor cells by T-VEC can induce an antiviral immune response that could eliminate tumor cells and hence improve T-VEC treatment efficacy (see Figure 3b). The sensitivity of all model parameters on the susceptible tumor cell population based on different trial durations (i.e., 1 month, 2 months, and 4 months) is shown in Figure 3a. The burst size of infected cells, b_T, and the rate at which new resting innate immune cells arrive in the tumor microenvironment *source of the resting innate immune cells* (S_{ZR}) gain significance as the duration of the clinical trial increases. The sensitivity coefficient of both b_T and S_{ZR} were not deemed to be clinically significant as their absolute values were <0.5.

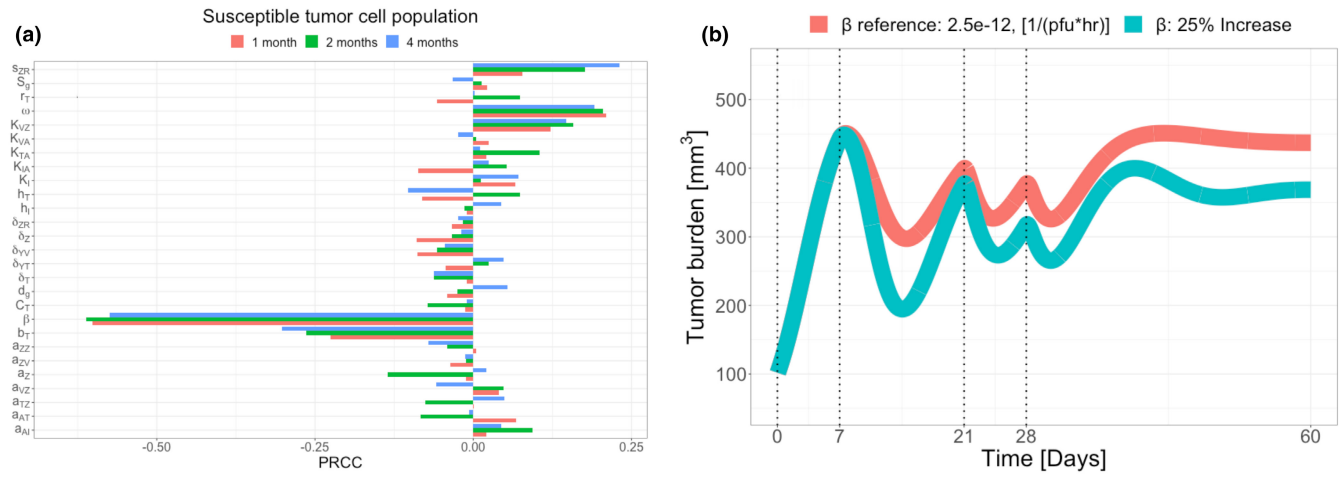

FIGURE 3 Model parameters affecting tumor burden. (a) Model parameter sensitivity affecting the susceptible tumor cell population based on a trial duration of 1 month, 2 months, and 4 months; (b) impact of viral infection rate β on tumor burden. a_{AI}, rate of infected cell mediated proliferation of virus specific adaptive immune cells; a_{AT}, rate of tumor cell mediated proliferation of tumor specific adaptive immune cells; a_{TZ}, activation rate of tumor specific adaptive immune cells via immune cells; a_{ZV}, virus mediated activation rate of resting innate immune cells; a_{ZZ}, activation of resting innate cells by previously activated innate immune cells; b_T, burst size of infected cells; β, viral infection rate; C_T, tumor cells carrying capacity; dg, GM-CSF clearance; δ_T, death rate of infected tumor cells; δ_{YT}, death rate of tumor specific adaptive immune cells; δ_{YV}, death rate of virus specific adaptive immune cells; δ_Z, death rate of innate immune cells; δ_{ZR}, death rate of resting innate immune cells; h_I, half saturation constant of infected tumor cells; h_T, half saturation constant of tumor cells; K_I, killing rate of infected cells by innate immune cells; K_{IA}, killing rate of infected cells by virus specific adaptive immune cells; K_{TA}, killing rate of tumor cells by tumor specific adaptive immune cells; K_{VA}, killing rate of T-VEC virions by virus-specific adaptive immune cells; K_{VZ}, killing rate of T-VEC virions by innate immune cells; PRCC, partial rank correlation coefficient; r_T, intrinsic tumor cell growth rate; S_g, GM-CSF proliferation rate; S_{ZR}, source of the resting innate immune cells; and ω, viral clearance rate.

On the systemic level, the source of the resting innate immune cells, S_{ZR}, and the death rate of innate immune cells, δ_Z, strongly impact the total number of available T-VEC viruses and the immune system with the strongest impact on the innate immune system. We have used the ratio between S_{ZR}/death rate of innate immune cells (δ_Z) as metric to assess if the innate immune system plays an inhibiting or stimulatory role on T-VEC treatment efficacy. If $S_{ZR}/\delta_Z > 1$ (i.e., $S_{ZR} > \delta_Z$), the rate at which new resting innate immune cells arrive in the tumor microenvironment is higher than the death rate of innate immune cells, indicating a well-functioning innate immune system. To showcase how the ratio $S_{ZR} > \delta_Z$ could influence T-VEC treatment efficacy, simulations of a subject administered with 10^6 pfu/ml of T-VEC at Day 7 followed by 10^8 pfu/ml at Days 21 and 33 were performed with and without a twofold increase of the S_{ZR}/δ_Z ratio. Figure 4 illustrates the findings. Figure 4a shows how an increase of $S_{ZR} > \delta_Z$ by twofold increases the number of innate immune cells. A high number of innate immune cells reduces the total number of available T-VEC viruses in the system as shown in Figure 4b and hence reduces T-VEC ability to reduce tumor burden (see Figure 4c). This result agrees with Eftimie and Eftimie,[16] who found a strong correlation between the total number of innate immune cells and tumor elimination. S_{ZR} was also found to be sensitive to both Y_T and Y_V, however the sensitivity coefficients were <0.5 and therefore not deemed clinically significant.

Simulations to quantify the dose–efficacy relationship of T-VEC

One of the objectives of developing the current viral kinetic mechanistic model was to develop a model to be used as a quantitative knowledge platform to accurately predict T-VEC treatment responses in future clinical trials. This was evaluated by assessing both the ability and the robustness of the viral kinetic model to predict realistic dose–efficacy relationships at the population level. The waterfall plot in Figure 5a and the table in Figure 5b show the distribution of responders according to RECIST categories[19] in a virtual population of 500 patients who were given the higher dose T-VEC regimen described previously. To assess the stability of the obtained distribution of the responders, 250 and 1000 virtual patients treated with T-VEC were simulated using the higher dose regimen. The distribution of percent of responders from 250, 500, and 1000 virtual patients were compared between the different populations and with observed data from the phase II single-arm, open-label study that evaluated the biodistribution and shedding of T-VEC in patients with unresected stage IIIB to IVM1c melanoma described previously and in the literature.[12] Figure 6a and Table S2 summarize these findings. Overall, the prediction of percentage of responders using RECIST criteria was stable and in agreement with the published values reported by Andtbacka et al.[12] Figure 6b presents the dose–response relationship between 500 virtual patients treated with T-VEC with the higher dose and lower dose regimens as described previously. Overall, the relationship between T-VEC doses and its efficacy suggests that an increase of ~10^2 pfu/ml 21 days and beyond after the initial dose of T-VEC resulted in an ~12% increase in response to T-VEC treatment in the patient population receiving the higher dose regimen compared with the lower dose regimen.

DISCUSSION

Common clinical pharmacology concepts that evaluate the safety and efficacy of small or large molecules cannot

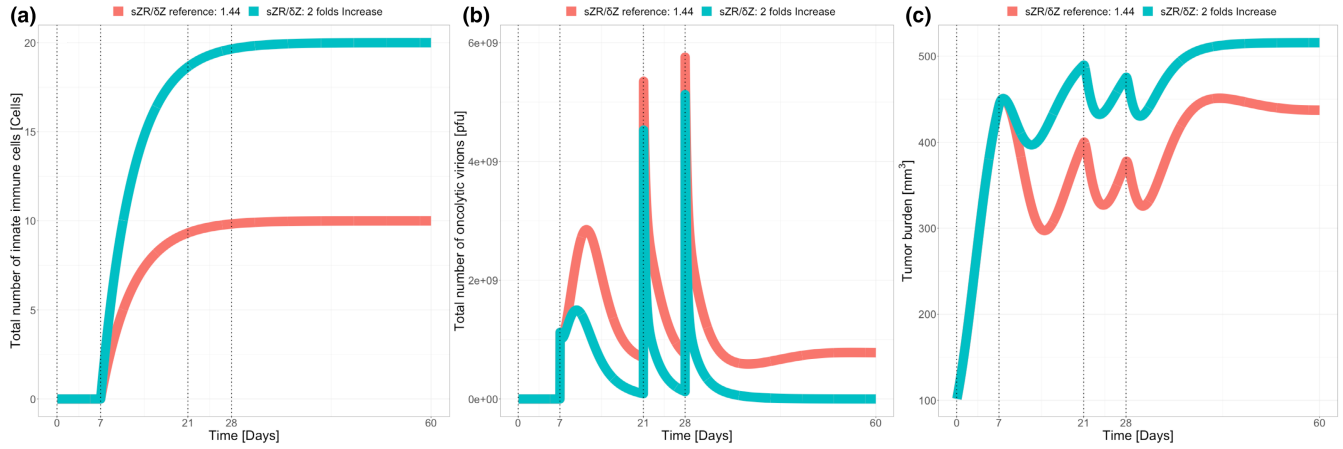

FIGURE 4 Impact of the innate immune system on tumor burden. (a) A twofold increase of sZR/δZ triggers strong innate immune system responses; (b) the reduction of Talimogene Laherparepvec (T-VEC) virion cells as result of a strong innate immune system response; and (c) the increase of tumor burden due to a reduction of T-VEC virion cells in the system. S_{ZR}/δ_Z, metric assessing the role of innate immune system on T-VEC treatment efficacy.

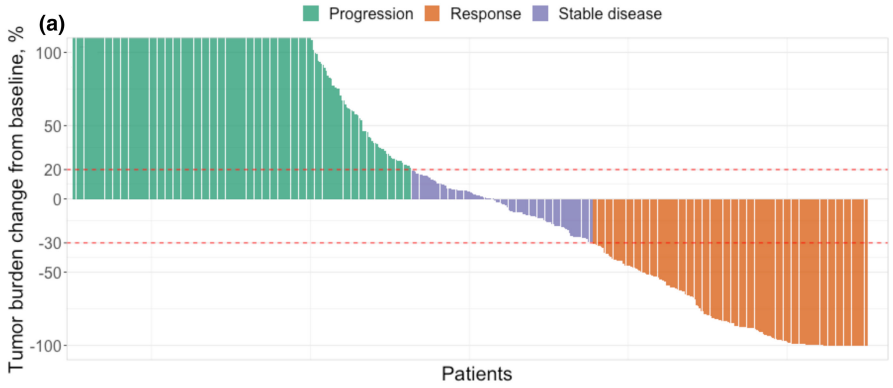

(b)

Overall Response	% Response rate (95% CI)	Number of Simulated Subjects
Progression	42.6 (38.0, 47.5)	213
Stable Disease	22.8 (18.2, 27.7)	114
Response	34.6 (30.0, 39.5)	173
Total	100%	500

FIGURE 5 Distribution of Talimogene Laherparepvec responders based on 500 virtual patients given the higher dose regimen. (a) Waterfall plot illustrating the distribution of tumor burden of simulated patients. Progression (progressive disease) is defined as a percentage change from baseline in tumor burden ≥20%, stable disease is defined as a 20% > percentage change from baseline in tumor burden ≥−30%, and response (partial or complete response) is defined as a −30% > percentage change from baseline in tumor burden. Baseline is defined as the tumor burden measurement at Day 7. (b) Table showing the proportion of patients in each category as shown in the waterfall plot (a). CI, confidence interval.

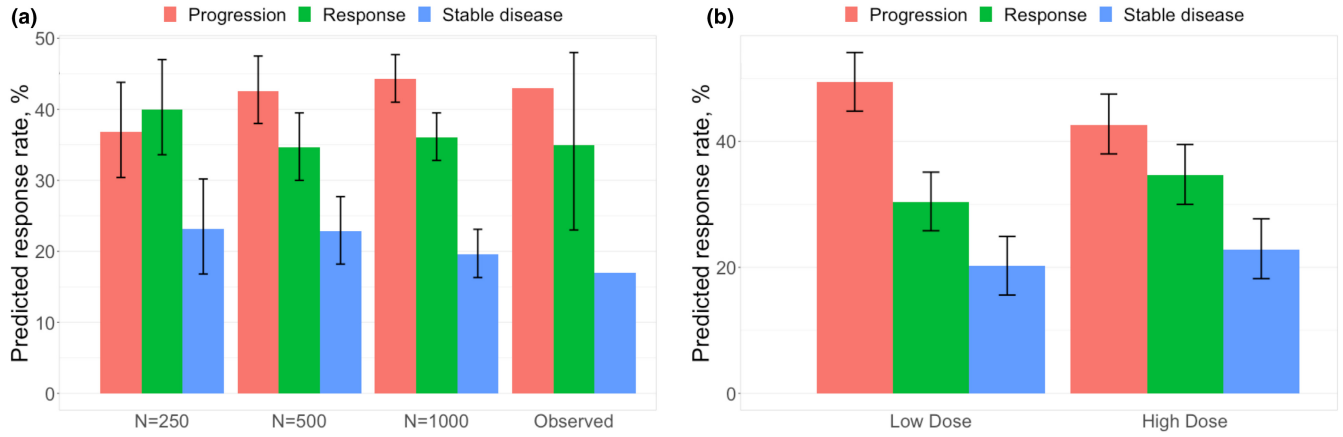

FIGURE 6 Simulation for patients given the higher dose regimen stratified by Response Evaluation Criteria in Solid Tumors category.[22] (a) Robustness of simulation platform. Observed data are as reported in Andtbacka et al.[12] Note that the "Observed" category responders and stable disease patients do not have 95% confidence intervals as these were not provided in Andtbacka et al.[12] Please see Table S1 for the distribution of patients in each category. (b) Comparisons of dose–response relationships between patients given high dose and low dose regimens. In all plots, progression is defined as percentage change from basline in tumor burden ≥20%, stable disease is defined as a 20% > percentage change from baseline in tumor burden ≥−30%, and response is defined as −30% > percentage change from baseline in tumor burden. Baseline is the tumor burden measurement at Day 7.

be applied to T-VEC.[25,26] Based on our best knowledge, a comprehensive quantitative approach that systematically evaluates the T-VEC treatment efficacy has not been developed yet. The current analysis aims to address this scientific gap by developing a viral kinetic mechanistic model that systematically evaluates T-VEC treatment efficacy. The developed viral kinetic mechanistic model adequately captures the well-known, complex, multifaceted mechanism of action of oncolytic viral therapy and incorporates specific characteristics of T-VEC, such as the interaction between GM-CSF, innate and adaptive immune responses, and the impact on treatment

efficacy, significantly extending previously published models.[12,13,27]

Global sensitivity analysis was performed to identify model parameters that could significantly influence T-VEC treatment efficacy. The results from the global sensitivity analysis suggested that viral infection rate β is one of the key parameters that drive treatment efficacy, which agrees with previously published literature.[14,15] On the systemic level, our global sensitivity analysis found that the dynamic interaction between T-VEC and innate immune system plays an important role. Specifically, a high ratio between the rate at which new resting innate immune cells arrive in the tumor microenvironment and the death rate of innate immune cells results in a strong innate immune system that reduces the amount of T-VEC in the system and in return reduces treatment efficacy. These findings are in alignment with the current understanding of the dynamic interactions between virotherapy and the immune system.[16]

Findings from OPTiM, a randomized, phase III, open-label trial,[12] demonstrated an increase of survival for patients with early metastatic melanoma (stage IIIB–IVM1a) treated with T-VEC compared with those treated with GM-CSF alone. Interestingly, several studies confirm that an overexpression of GM-CSF leads to severe inflammation.[28–30] Currently, no quantitative understanding on how the activation of GM-CSF could impact T-VEC treatment efficacy exists. To address this knowledge gap, correlations between parameters related to GM-CSF activation and responders to T-VEC treatment were quantified. Our simulation results found that T-VEC responders have a lower GM-CSF activation rate compared with nonresponders (see Figure 7a). This finding suggests that the overexpression of GM-CSF could negatively impact T-VEC treatment efficacy, which is in line with the current understanding of the immunobiology of GM-CSF in T cell responses.[5] Figure 7b quantifies at which degree the increase of GM-CSF activation rate would affect tumor burden. Our simulation has shown that an increase of greater that ~10-fold of the value of the activation rate could increase tumor burden, although the clinical significance of this change is doubtful.

Finally, findings from a series of clinical trial simulations assessing the robustness and precision in quantifying the relationship between two different T-VEC dosing regimens and T-VEC treatment efficacy confirmed our confidence in the developed model to be used as a quantitative knowledge-based platform for future oncolytic molecules.

One of the limitations of the current analysis was the limited clinical biodistribution data available for the model development. Implementation of additional biodistribution data together with longitudinal tumor volume in the future could improve the prediction of the current analysis. Furthermore, most of the systematic model parameters were borrowed from animal models (see the Data S1), and it is not clear how these parameters translate to humans. However, our detailed analysis and simulations confirmed that our findings are strongly correlated with the current understanding of the T-VEC mechanism of action and confirm the validity of the values of the model parameters that being used in the current model.

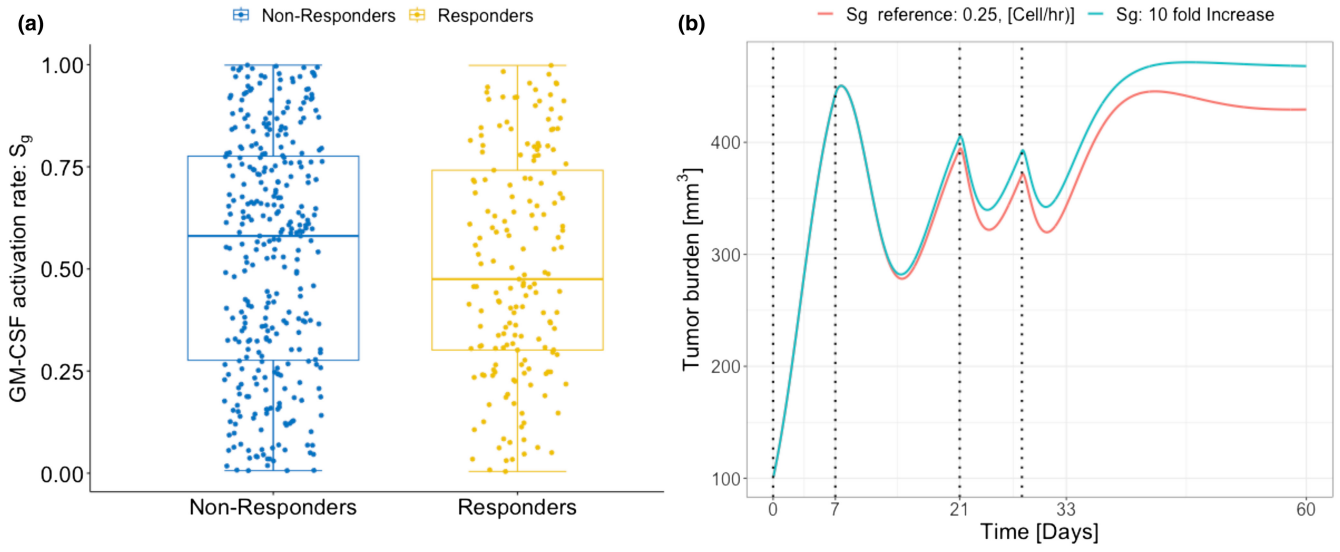

FIGURE 7 Impact of granulocyte-macrophage colony-stimulating factor (GM-CSF) activation rate on tumor burden. (a) Correlation between distribution of GM-CSF activation rate with responders/nonresponders. Note that here "responders" included patients with progression or stable disease as defined by Response Evaluation Criteria in Solid Tumors category.[22] (b) Impact of a 10-fold increase of GM-CSF activation rate on tumor burden. S_g, GM-CSF proliferation rate

In summary, this platform model adequately captures the well-known, complex, multifaceted mechanism of action of oncolytic viral therapy and identifies under which condition the immune system either assists in eliminating tumor cells or inhibits T-VEC efficacy, which is critical to both efficiently design future oncolytic agents and understand cancer development.

AUTHOR CONTRIBUTIONS

M.A., J.K., and V.V.U. wrote the manuscript. M.A., J.K., X.H., S.D., and V.V.U. designed the research. M.A., J.K., and P.-W.C. performed the research. M.A. and P.-W.C. analyzed the data.

ACKNOWLEDGMENTS

The authors thank the patients and their families and caregivers for participating in this study; and Adimoolam Narayanan, a previous employee of Amgen Inc (Thousand Oaks, CA) currently at Amador Bioscience (Pleasanton, CA), for technical support.

FUNDING INFORMATION

Funding was provided by Amgen Inc, Thousand Oaks, CA.

CONFLICT OF INTEREST

All authors are employees of the stated companies.

ORCID

Johannes Kast https://orcid.org/0000-0001-8963-8972
Vijay V. Upreti https://orcid.org/0000-0003-1018-7166

REFERENCES

1. de Matos AL, Franco LS, McFadden G. Oncolytic viruses and the immune system: the dynamic duo, molecular therapy. *Meth Clin Dev*. 2020;17:349-358.
2. Filley AC, Dey M. Immune system, friend or foe of oncolytic Virotherapy? *Front Oncol*. 2017;7:106.
3. Parato KA, Senger D, Forsyth PAJ, Bell JC. Recent progress in the battle between oncolytic viruses and tumours. *Nat Rev Cancer*. 2005;5:12.
4. Liu TC, Galanis E, Kirn D. Clinical trial results with oncolytic virotherapy: a century of promise, a decade of progress. *Nat Clin Pract Oncol*. 2007;4:2-117. doi:10.1038/ncponc0736
5. Shi Y, Liu CH, Roberts AI, et al. Granulocyte-macrophage colony-stimulating factor (GM-CSF) and T-cell responses: what we do and don't know. *Cell Res*. 2006;16:126-133.
6. Burgess AW, Camakaris J, Metcalf D. Purification and properties of colony-stimulating factor from mouse lung-conditioned medium. *J Biol Chem*. 1977;252:1998-2003.
7. Burgess AW, Metcalf D. The nature and action of granulocyte macrophage colony stimulating factors. *Blood*. 1980;56:947-958.
8. Nicola NA. Granulocyte colony-stimulating factor and differentiation-induction in myeloid leukemic cells. *Int J Cell Cloning*. 1987;5:1-15.
9. Robert M. Conry, Brian Westbrook, Svetlana McKee, and Timothy Graham Norwood, Talimogene laherparepvec: first in class oncolytic virotherapy. *Hum Vaccin Immunother*. 2018;14:839-846.
10. Kohlhapp FJ, Kaufman HL. Molecular pathways: mechanism of action for talimogene laherparepvec, a new oncolytic virus immunotherapy. *Clin Cancer Res*. 2015;22(5):1048-1054.
11. Hu JC, Coffin RS, Davis CJ, et al. A phase I study of OncoVEXGM-CSF, a second-generation oncolytic herpes simplex virus expression granulocyte macrophage colony-stimulating facot. *Clin Cancer Res*. 2006;12(22):6737-6747.
12. Andtbacka RHI, Amatruda T, Nemunaitis J, et al. Biodistribution, shedding, and transmissibility of the oncolytic virus talimogene laherparepvec in patients with melanoma. *EBioMedicine*. 2019;47:89-97.
13. Andtbacka RHI, Ross M, Puzanov I, et al. Patterns of clinical response with talimogene laherparepvec (T-VEC) in patients with melanoma treated in the OPTiM phase III clinical trial. *Ann Surg Oncol*. 2016;23(13):4169-4177.
14. Mahasa KJ, Eladdadi A, de Pillis L, Ouifki R. Oncolytic potency and reduced virus tumor specificity in oncolytic virotherapy. A mathematical modelling approach. *PLoS ONE*. 2017;12(9):e0184347.
15. Storey KM, Lawler SE, Jackson TL. Modeling oncolytic viral therapy, immune checkpoint inhibition, and the complex dynamics of innate and adaptive immunity in glioblastoma *treatment*. *Front Physiol*. 2020;11:151.
16. Eftimie R, Eftimie G. Tumour-associated macrophages and oncolytic virotherapies: a mathematical investigation into a complex dynamic. *Letters in Biomathematics*. 2018;5(S1):S6-S35.
17. Eftimie R, Dushoff J, Bridle B, Bramson J, Earn D. Multistability and multi-instability phenomena in a mathematical model of tumor-immune-virus interactions. *Bull Math Biol*. 2011;73:2932-2961.
18. Wu JT, Byrne HM, Kirn DH, Wein LM. Modeling and analysis of a virus that replicates selectively in tumor cells. *Bull Math Biol*. 2001;63(4):731-768.
19. Paiva LR, Binny C, Ferreira SC, Martins ML. A multiscale mathematical model for oncolytic virotherapy. *Cancer Res*. 2009;69(3):1205-1211.
20. de Pillis LG, Radunskaya AE, Wiseman CL. A validated mathematical model of cell-mediated immune response to tumour growth. *Cancer Res*. 2005;65(17):7950-7958.
21. Titze MI, Frank J, Ehrhardt M, Smola S, Graf N, Lehr T. A generic viral dynamic model to systematically characterize the interaction between oncolytic virus kinetics and tumor growth. *Eur J Pharm Sci*. 2017;97:38-46.
22. Eisenhauer EA, Therasse P, Bogaerts J, et al. New response evaluation criteria in solid tumours: revised RECIST guideline (version 1.1). *Eur J Cancer*. 2009;45(2):228-247.
23. Chalom A, Prado PIKL. Parameter space exploration of ecological models, arXiv:1210.6278 [q-bio.QM], 2012.
24. Chalom A, Mandai C, Prado P. sensitivity analyses: a brief tutorial with R package pse. *R Package*. 2013;25 version 0.3.1.
25. Belov A, Schultz K, Forshee R, Tegenge MA. Opportunities and challenges for applying model-informed drug development approaches to gene therapies. *CPT Pharmacometrics Syst Pharmacol*. 2021;10:286-290.
26. Wang Y, Zhu H, Madabushi R, Liu Q, Huang SM, Zineh I. Model-informed drug development: current us regulatory

practice and future considerations. *Clin Pharmacol Ther*. 2019;105(4):899-911.
27. Andtbacka RHI, Kaufman HL, Collichio F, et al. Talimogene Laherparepvec improves durable response rate in patients with advanced melanoma. *J Clin Oncol*. 2015;33(25):2780-2788.
28. Lang RA, Metcalf D, Cuthbertson RA, et al. Transgenic mice expressing a hemopoietic growth factor gene (GM-CSF) develop accumulations of macrophages, blindness, and a fatal syndrome of tissue damage. *Cell*. 1987;51:675-686.
29. Alderuccio F, Biondo M, Toh BH. Organ-specific autoimmunity in granulocyte macrophage-colony stimulating factor (GM-CSF) deficient mice. *Autoimmunity*. 2002;35:67-73.
30. Biondo M, Nasa Z, Marshall A, Toh BH, Alderuccio F. Local transgenic expression of granulocyte macrophage-colony stimulating factor initiates autoimmunity. *J Immunol*. 2001;166:2090-2099.

SUPPORTING INFORMATION

Additional supporting information can be found online in the Supporting Information section at the end of this article.

How to cite this article: Ahamadi M, Kast J, Chen P-W, Huang X, Dutta S, Upreti VV. Oncolytic viral kinetics mechanistic modeling of Talimogene Laherparepvec (T-VEC) a first-in-class oncolytic viral therapy in patients with advanced melanoma. *CPT Pharmacometrics Syst Pharmacol*. 2023;12:250-260. doi:10.1002/psp4.12898